

Entanglement and correlation functions following a local quench: a conformal field theory approach

Pasquale Calabrese¹ and John Cardy²

¹Dipartimento di Fisica dell'Università di Pisa and INFN, Pisa, Italy.

²Oxford University, Rudolf Peierls Centre for Theoretical Physics, 1 Keble Road, Oxford, OX1 3NP, United Kingdom and All Souls College, Oxford.

Abstract. We show that the dynamics resulting from preparing a one-dimensional quantum system in the ground state of two decoupled parts, then joined together and left to evolve unitarily with a translational invariant Hamiltonian (a local quench), can be described by means of quantum field theory. In the case when the corresponding theory is conformal, we study the evolution of the entanglement entropy for different bi-partitions of the line. We also consider the behavior of one- and two-point correlation functions. All our findings may be explained in terms of a picture, that we believe to be valid more generally, whereby quasiparticles emitted from the joining point at the initial time propagate semiclassically through the system.

1. Introduction.

The understanding of the degree of entanglement in extended quantum systems has prompted an enormous effort in a field at the border of condensed matter physics, quantum information theory, and quantum field theory. It would take too long to mention all the topics and problems addressed so far: we refer the reader to a recent thorough review and extensive bibliography [1].

Several measures have been introduced to quantify the entanglement in an extended system [1]. Among them we consider here only the entanglement entropy, which is defined as follows. Suppose a whole system is in a pure quantum state $|\Psi\rangle$, with density matrix $\rho = |\Psi\rangle\langle\Psi|$, and an observer A measures only a subset A of a complete set of commuting observables, while another observer B may measure the remainder. A's reduced density matrix is $\rho_A = \text{Tr}_B \rho$. The entanglement entropy is just the von Neumann entropy

$$S_A = -\text{Tr}_A \rho_A \log \rho_A \quad (1)$$

associated with this reduced density matrix. For an unentangled product state, $S_A = 0$. Conversely, S_A should be a maximum for a maximally entangled state. One of the most striking features of the entanglement entropy is its universal behavior displayed at and close to a quantum phase transition. In fact, close to a quantum critical point, where the correlation length ξ is much larger than the lattice spacing a , the long-distance behavior of the correlations in the ground state of a quantum spin chain are effectively described by a 1+1 dimensional quantum field theory. At the critical point, where ξ diverges, the field theory, if Lorentz invariant, is also a *conformal* field theory (CFT). In the latter case, it has been shown that, if A is an interval of length ℓ in an infinite chain, $S_A \simeq (c/3) \log \ell$ [2, 3, 4], where c is the central charge of the corresponding CFT. When the correlation length ξ is large but finite (more precisely $\xi \ll \ell$), it has been shown that, increasing ℓ , S_A saturates [3] to $S_A \simeq (c/3) \log \xi$ [4, 5].

Recently the interest in the properties of entanglement has been extended to understanding its dynamical behavior. The natural question is how the entanglement propagates through the system when it is prepared in a state that is not an eigenstate and then is left to evolve in the absence of any dissipation. The most common situation studied so far concerns a sudden quench of some coupling of the model Hamiltonian [6, 7, 8, 9, 10]. The main motivation for the large number of studies of this dynamics is that it may actually be realized and measured in ultra-cold atomic systems [11]. For a complete list of references on the subject we refer to our earlier paper [12].

Here we consider a different situation, known in the literature as local quench [13]. We will concentrate on the case when a physical one-dimensional system (e.g. a spin chain) is physically cut into two parts that are in their own ground state. We then join the two halves at a given time $t = 0$ and study the subsequent evolution according to a translational invariant hamiltonian. Here, the entanglement entropy is the most natural quantity to be studied because the two halves are clearly unentangled for $t < 0$ whereas the initial energy differs from that of the ground state only by a finite amount. This differs from the case of a global quench, when the energy of the initial state above the ground state is always extensive, and correspondingly the entanglement can be extensively larger. We will only consider gapless models that are described asymptotically by a boundary CFT, since in this case we can use powerful analytic results [14, 15].

The paper is organized as follows. In Sec. 2 we briefly recall the CFT approach to the entanglement entropy. We outline the setup for the local quench which is then applied to different situations in the following section 3. Then we consider the time evolution of correlation functions in Sec. 4. In Sec. 5 we describe how this approach can be generalized to the case with two joining points and we derive an heuristic solution. Finally we conclude the paper with a discussion of open problems and possible generalizations in Sec. 6.

2. The CFT approach to entanglement entropy and a local quench

2.1. Entanglement entropy and CFT

The entanglement entropy S_A defined by Eq. (1) can be studied in a general quantum field theory through the replica trick [4]

$$S_A = -\frac{\partial}{\partial n} \text{Tr} \rho_A^n \Big|_{n=1}. \quad (2)$$

This is particular useful in a CFT because, when A consists of disjoint intervals with N boundary points with B , $\text{Tr} \rho_A^n$ transforms under a general conformal transformation as the N point function of a primary field Φ_n with conformal dimension [4]

$$x_n = \frac{c}{12} \left(n - \frac{1}{n} \right), \quad (3)$$

where c is the central charge of the underlying CFT.

In particular this implies that the entanglement entropy of a slit of length ℓ in an infinite system is given by

$$\text{Tr} \rho_A^n = c_n \left(\frac{\ell}{a} \right)^{-2x_n} \Rightarrow S_A = \frac{c}{3} \log \frac{\ell}{a} + c'_1, \quad (4)$$

where a is an UV cutoff (e.g. in a spin chain is the lattice spacing). The constants c_n are also non-universal and so is the derivative for $n = 1$, c'_1 , entering in S_A . However, in any particular model, a and c'_1 can be fixed unambiguously by specific requirements (see e.g. [5]).

Another important result we will use in the following is the entanglement of the slit $A = [0, \ell]$ in a semi-infinite line with specific boundary conditions at $r = 0$, that is given by [4]

$$\text{Tr} \rho_A^n = \tilde{c}_n \left(\frac{2\ell}{a} \right)^{-x_n} \Rightarrow S_A = \frac{c}{6} \log \frac{2\ell}{a} + \tilde{c}'_1. \quad (5)$$

In analogy to the c_n , the constants \tilde{c}_n are not universal and depend on the boundary condition at $r = 0$. However comparing the finite temperature result of Ref. [4] with the standard thermodynamic entropy for systems with boundaries [16] we have [4, 17, 18]

$$\tilde{c}'_1 - c'_1/2 = \log g, \quad (6)$$

where $\log g$ is the boundary entropy first introduced by Affleck and Ludwig [16]. We recall that g is universal and depends only on the boundary CFT.

2.2. CFT for global quenches

CFT is also able to predict the time-dependence of the entanglement entropy after a global quench [6]. We briefly summarize here these results, because some of them will be useful in understanding the local case. The density matrix has the path integral representation [6]

$$\langle \psi''(r'') | \rho(t) | \psi'(r') \rangle = Z_1^{-1} \langle \psi''(r'') | e^{-itH - \epsilon H} | \psi_0(r) \rangle \langle \psi_0(r) | e^{+itH - \epsilon H} | \psi'(r') \rangle, \quad (7)$$

where we included damping factors $e^{-\epsilon H}$ in such a way as to make the path integral absolutely convergent. Each of the factors may be represented by an analytically continued path integral in imaginary time: the first one over fields $\psi(r, \tau)$ which take the boundary values $\psi_0(r)$ on $\tau = -\epsilon - it$ and $\psi''(r)$ on $\tau = 0$, and the second with $\psi(r, \tau)$ taking the values $\psi'(r)$ on $\tau = 0$ and $\psi_0(r)$ on $\tau = \epsilon - it$. When H is critical and the field theory is a CFT, under the renormalization group any *translationally* invariant boundary condition is supposed to flow into a boundary fixed point, satisfying conformal boundary conditions. Thus we may assume that the state $|\psi_0\rangle$ corresponds to such boundary conditions on sufficiently long length scales. Thus, for real τ , the strip geometry described above may be obtained from the upper half-plane (where the entanglement entropy is known from [4]) by the conformal mapping $w = (2\epsilon/\pi) \log z$. In this way one easily get the result for imaginary time. The real time evolution is obtained by continuing $\tau = \epsilon + it$. The final result is [6]

$$S_A(t) \simeq \begin{cases} \frac{\pi ct}{6\epsilon} & t < \ell/2, \\ \frac{\pi c \ell}{12\epsilon} & t > \ell/2. \end{cases} \quad (8)$$

From this we note that ϵ enters in the calculation in an essential way. A careful analysis [19, 12] shows that in fact it corresponds to the correlation length in the initial state and so it is not only a useful tool, but a physical important parameter.

The fact that $S_A(t)$ increases linearly until it saturates at $t^* = \ell/2$ has a simple interpretation in terms of quasiparticles excitations emitted from the initial state at $t = 0$ and freely propagating with velocity $v = 1$. This phenomenon is very general and holds even for non-critical systems, and it has been confirmed by exactly integrable dynamics and numerics (see e.g. [6, 7, 13]) However, since in lattice models there are particles moving slower than v , after t^* the entropy does not saturate abruptly, but is a slowly increasing function of the time. The same picture is valid for the correlation functions. Firstly incoherent quasi-particles arriving a given point from well-separated sources cause relaxation of (most) local observables towards their ground-state expectation values. Secondly, entangled quasiparticles (emitted from an initially correlated region) arriving at the same time t induce correlations between local observables. In the case where they travel at a unique speed v , therefore, there is a sharp ‘‘horizon’’ effect: the connected correlations do not change significantly from their initial values until time $t \sim |r|/2v$. After this they rapidly saturate to time-independent values. For large separations, these decay exponentially differently from the power law dependence in the ground state. Also for correlation functions, this picture has been shown to be valid in several models (see e.g. [19, 12, 20, 21, 22, 23]).

It is clear that a very similar interpretation should apply also for local quenches, but with the fundamental difference that now the quasi-particle excitations are emitted only from the point where the quench happened and not from everywhere.

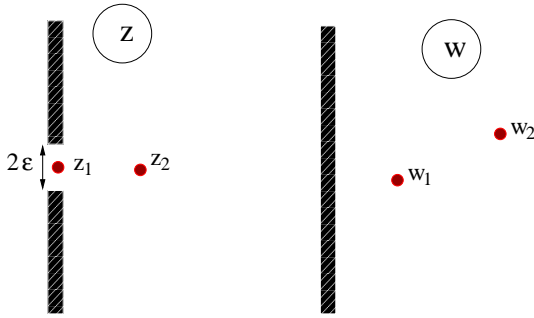


Figure 1. Space-time region for the density matrix (left) mapped to the half-plane (right) by means of Eq. (9). $z_1 = i\tau$ and $z_2 = i\tau + \ell$ during the computation and in the end $\tau \rightarrow it$.

2.3. CFT setup for local quenches

Suppose we physically cut a spin chain at the boundaries between two subsystems A and B, and prepare a state where the individual pieces are in their respective ground states. In this state the two subsystems are completely unentangled, and its energy differs from that of the ground state by only a finite amount. Let us join up the pieces at time $-t$ and watch the system evolve up to $t = 0$.

The procedure for the global quenches does not apply because the initial state is not translational invariant and will not flow under the renormalization group toward a conformally invariant boundary state. One may try to handle the problem introducing proper boundary condition changing operators (see e.g. [24]). However we prefer to take a different approach. In fact, we can simply represent the corresponding density matrix in terms of path integral on a modified world-sheet. The physical cut corresponds to having a slit parallel to the (imaginary) time axis, starting from $-\infty$ up to $\tau_1 = -\epsilon - it$ (the time when the two pieces have been joined), and analogously the other term of the density matrix, like in Eq. (7), gives a slit from $\tau_2 = \epsilon - it$ to $+\infty$. Again we introduced the regularization factor ϵ , that we will interpret a posteriori.

For computational simplicity we will consider the translated geometry with two cuts starting at $\pm i\epsilon$ and operator inserted at imaginary time τ . This should be considered real during the course of all the computation, and only at the end can be analytically continued to it . This plane with the two slits is pictorially represented on the left of Fig. 1 where $i\tau$ corresponds to z_1 . As shown in the same figure, the z -plane is mapped into the half-plane $\text{Re } w > 0$ by means of the conformal mapping

$$w = \frac{z}{\epsilon} + \sqrt{\left(\frac{z}{\epsilon}\right)^2 + 1} \quad \text{with inverse} \quad z = \epsilon \frac{w^2 - 1}{2w}. \quad (9)$$

On the two slits in the z plane (and so on the imaginary axis in the w one) conformal boundary conditions compatible with the initial state must be imposed. For example, in the most natural situation when the boundary “spins” are left free, we require free boundary conditions. Oppositely, when the boundary spins are supposed to stay in a particular state we require fixed boundary conditions.

Note that this setting is valid in any dimension when the system is prepared in two spatially divided halves. In this case one can try to tackle the problem with the methods of boundary critical phenomena [25], but this will be extremely difficult, if not impossible, since conformal invariance is far less powerful.

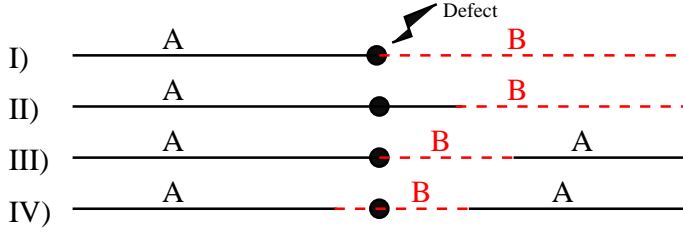


Figure 2. The four different bipartitions of the line we consider here.

3. Entanglement entropy

In this section we consider the time evolution of the entanglement entropy after the local quench. We consider two half-chains joined together at the point $r_D = 0$ at a given time. The various subcases we consider correspond to different spatial partitions of the system among which we calculate the entanglement. We consider the four different situations depicted in Fig. 2.

We start with the more natural division, considering the entanglement entropy between the two parts in which the system was divided before the quench (case I). As case II we consider the entanglement of the region $r > \ell$ with $r < \ell$. This will allow us to identify simple horizon effects. To highlight the interaction of the two previous effects we then consider the entanglement of the part $B = [0, \ell]$ with the rest (case III). Finally we consider as IV the most general slit $B = [\ell_1, \ell_2]$. Clearly cases I and III are particular choices of II and IV respectively and can be derived as simple limits. However we prefer to present the results in such order because the physical effects and their interpretation will emerge in a more natural way.

3.1. Case I: Entanglement of the two halves

This is the case when B is the positive real axis and A is the negative real axis. $\text{Tr} \rho_A^n$ transforms like a one-point function that in the w plane is $[2\text{Re}w_1]^{-x_n}$. Thus in the z plane at the point $z_1 = (0, i\tau)$ we have

$$\langle \Phi_n(z_1) \rangle = \tilde{c}_n \left(\left| \frac{dw}{dz} \right|_{z_1} \frac{a}{[2\text{Re}w_1]} \right)^{x_n} \quad (10)$$

that using

$$\epsilon w_1 = i\tau + \sqrt{\epsilon^2 - \tau^2}, \quad \left| \frac{dw}{dz} \right|_{z_1} = \frac{\epsilon}{\sqrt{\epsilon^2 - \tau^2}}, \quad (11)$$

becomes

$$\langle \Phi_n \rangle = \tilde{c}_n \left(\frac{a\epsilon/2}{\epsilon^2 - \tau^2} \right)^{x_n}. \quad (12)$$

Continuing this result to real time $\tau \rightarrow it$ we obtain

$$\langle \Phi_n(t) \rangle = \tilde{c}_n \left(\frac{a\epsilon/2}{\epsilon^2 + t^2} \right)^{x_n}. \quad (13)$$

Using finally the replica trick to find the entanglement entropy we have

$$S_A = - \frac{\partial}{\partial n} \text{Tr} \rho_A^n \Big|_{n=1} = \frac{c}{6} \log \frac{t^2 + \epsilon^2}{a\epsilon/2} + \tilde{c}'_1. \quad (14)$$

There are two main pieces of information that we can extract from this result, coming from the long and the short time behavior. For $t \gg \epsilon$ we have

$$S_A(t \gg \epsilon) = \frac{c}{3} \log \frac{t}{a} + k_0, \quad (15)$$

i.e. the leading long time behavior is only determined by the central charge of the theory in analogy with the ground state value for a slit. This could result in a quite powerful tool to extract the central charge in time-dependent numerical simulations. This behavior resembles the slow increasing of S_A observed numerically in Ref. [26] (unfortunately these data were never fitted, to understand the quantitative predictive power of our formula). The constant k_0 is given by $k_0 = \tilde{c}'_1 + (c/6) \log(2a/\epsilon)$.

The behavior for short time allows instead to fix the regulator ϵ in terms of the non-universal constant \tilde{c}'_1 . In fact we have

$$S_A(t = 0) = \frac{c}{6} \log \frac{2\epsilon}{a} + \tilde{c}'_1 = 0 \quad \Rightarrow \quad \epsilon = \frac{a}{2} e^{-6\tilde{c}'_1/c}. \quad (16)$$

Note that, even if non-universal, for a given lattice model the constant \tilde{c}'_1 can be fixed only by ground state quantities. Consequently Eq. (14) has no free dynamical parameter.

The parameter ϵ depends in a specific manner on the boundary contribution to the entanglement \tilde{c}'_1 . This is completely different from what happens for a global quench where the equivalent regulator is connected to the correlation length in the initial state [19, 12]. Furthermore the order of magnitude of ϵ is fixed by the lattice spacing a (i.e. the UV cutoff) and so considering the limit of times and lengths larger than ϵ is equivalent to the standard condition to apply the field theory for distances larger than a .

3.2. Case II: Decentered defect

Let us now consider the entanglement of the region $r > \ell$ with the rest of the system. In this case $\text{Tr} \rho_A^n$ is equivalent to the one-point function in the plane z at the point $z_2 = \ell + i\tau$ as in Fig. 1. Under the conformal mapping (1) this point goes into

$$\epsilon w_2 = \ell + i\tau + \sqrt{\epsilon^2 + (\ell + i\tau)^2} \equiv \ell + i\tau + \rho e^{i\theta} \quad (17)$$

with

$$\rho^2 = \sqrt{(\epsilon^2 + \ell^2 - \tau^2)^2 + 4\ell^2\tau^2}, \quad \theta = \frac{1}{2} \arctan \frac{2\ell\tau}{\sqrt{\epsilon^2 + \ell^2 - \tau^2}}, \quad (18)$$

and

$$\left| \epsilon \frac{dw}{dz} \right|_{z_2} = \frac{\sqrt{(\ell + \rho \cos \theta)^2 + (\tau + \rho \sin \theta)^2}}{\rho}. \quad (19)$$

Thus $\langle \Phi_n \rangle$ is given by Eq. (12) with $w_1 \rightarrow w_2$, resulting in

$$\langle \Phi_n \rangle = \tilde{c}_n \left(\frac{a \sqrt{(\ell + \rho \cos \theta)^2 + (\tau + \rho \sin \theta)^2}}{2\rho(\ell + \rho \cos \theta)} \right)^{x_n}. \quad (20)$$

The real time evolution for $t, \ell \gg \epsilon$ is obtained by analytically transforming $\tau \rightarrow it$. The calculation can seem very cumbersome, but it is greatly simplified by the fact

that in this limit we have $\rho^2 \rightarrow |\ell^2 - t^2|$ and $\rho \cos \theta \rightarrow \max[\ell, t]$, $\rho \sin \theta \rightarrow i \min[\ell, t]$. Care must also be taken when the zero-th order in ϵ is vanishing. In the end we have

$$\frac{\sqrt{(\ell + \rho \cos \theta)^2 + (\tau + \rho \sin \theta)^2}}{2\rho(\ell + \rho \cos \theta)} \rightarrow \begin{cases} \frac{1}{2|\ell|} & t < \ell, \\ \frac{\epsilon}{2(t^2 - \ell^2)} & t > \ell, \end{cases} \quad (21)$$

that leads to

$$S_A = \begin{cases} \frac{c}{6} \log \frac{2\ell}{a} + \tilde{c}'_1 & t < \ell, \\ \frac{c}{6} \log \frac{t^2 - \ell^2}{a^2} + k_0 & t > \ell, \end{cases} \quad (22)$$

with k_0 the same as in Eq. (15). The interpretation of this result is quite direct. Indeed at $t = 0$ the joining procedure produces a quasi-particle excitation at $r = 0$ that propagates freely with the corresponding speed of sound v_s that in the CFT normalization is $v_s = 1$. This excitation takes a time $t = \ell$ to arrive at the border between A and B and only at that time will start modifying their entanglement. The following evolution for $t \gg \ell$ is the same as in Eq. (15).

Also the constant value for $t < \ell$ deserves a comment: it is exactly the value known from CFT for the slit in the half-line Eq. (5). This is a non-trivial consistency check. Note that a finite ϵ smooths the crossover between the two regimes and makes the entanglement entropy a continuous function of the time.

3.3. Case III: The slit with the defect at the border

Let us consider again the same physical situation as before, but we now calculate the entanglement entropy of $A = [0, \ell]$ and B the remainder. For $t < 0$ the real negative axis is decoupled from the rest and does not contribute to the entanglement entropy, that is just the one of a slit in half-chain, i.e. the initial entropy is given by Eq. (5).

The entanglement entropy is obtained from the replica trick considering the scaling of a two-point function between the endpoints of the slit. In the z plane these two points are $z_1 = i\tau$ and $z_2 = \ell + i\tau$ (we adopt the same notation as before to make direct the use of previous formulas). As usual, the plane with cuts is mapped into the half-plane $\text{Re } w > 0$ by the transformation (9). On the w plane we have [4]

$$\langle \Phi_n(w_1) \Phi_{-n}(w_2) \rangle = \tilde{c}_n^2 \left(\frac{a^2 |w_1 + \bar{w}_2| |w_2 + \bar{w}_1|}{|w_1 - w_2| |\bar{w}_2 - \bar{w}_1| |w_1 + \bar{w}_1| |w_2 + \bar{w}_2|} \right)^{x_n}, \quad (23)$$

so the mapping to the original plane z is

$$\langle \Phi_n(z_1) \Phi_{-n}(z_2) \rangle = \tilde{c}_n^2 \left(\left| \frac{dw}{dz} \right|_{z_1} \left| \frac{dw}{dz} \right|_{z_2} \frac{a^2 |w_1 + \bar{w}_2| |w_2 + \bar{w}_1|}{|w_1 - w_2| |\bar{w}_2 - \bar{w}_1| |w_1 + \bar{w}_1| |w_2 + \bar{w}_2|} \right)^{x_n} \quad (24)$$

where the various terms are functions of z_i through Eqs. (11), (17), (18), (19), and

$$\epsilon^2 |w_1 - w_2|^2 = (\ell + \rho \cos \theta - \sqrt{\epsilon^2 - \tau^2})^2 + \rho^2 \sin^2 \theta, \quad (25)$$

$$\epsilon^2 |w_1 + \bar{w}_2|^2 = (\ell + \rho \cos \theta + \sqrt{\epsilon^2 - \tau^2})^2 + \rho^2 \sin^2 \theta. \quad (26)$$

Putting everything together we get

$$\langle \Phi_n(z_1 = i\tau) \Phi_{-n}(z_2 = \ell + i\tau) \rangle = \tilde{c}_n^2 \left(\frac{a^2 \epsilon}{\epsilon^2 - \tau^2} \frac{(\ell + \rho \cos \theta + \sqrt{\epsilon^2 - \tau^2})^2 + \rho^2 \sin^2 \theta}{(\ell + \rho \cos \theta - \sqrt{\epsilon^2 - \tau^2})^2 + \rho^2 \sin^2 \theta} \frac{\sqrt{(\ell + \rho \cos \theta)^2 + (\tau + \rho \sin \theta)^2}}{4\rho(\ell + \rho \cos \theta)} \right)^{x_n} \quad (27)$$

Again this simplifies considering the limit $t, \ell \gg \epsilon$ as explained after Eq. (20). We finally obtain

$$\text{Tr} \rho_A^n = \begin{cases} \tilde{c}_n^2 \left(\frac{a^2 \ell + t \epsilon}{t^2 \ell - t 4\ell} \right)^{x_n} & t < \ell, \\ \tilde{c}_n^2 \left(\frac{a^2}{\ell^2} \right)^{x_n} & t > \ell. \end{cases} \quad (28)$$

Note that for $t > \ell$ the calculation is slightly more cumbersome because we should take into account the first order in ϵ of some expressions.

Using finally the replica trick we get for the entanglement entropy

$$S_A = \begin{cases} \frac{c}{3} \ln \frac{t}{a} + \frac{c}{6} \ln \frac{\ell}{\epsilon} + \frac{c}{6} \ln 4 \frac{\ell - t}{\ell + t} + 2\tilde{c}'_1 & t < \ell, \\ \frac{c}{3} \ln \frac{\ell}{a} + 2\tilde{c}'_1 & t > \ell. \end{cases} \quad (29)$$

The crossover time $t^* = \ell$ is again in agreement with the quasi-particles interpretation.

There are several interesting features of this result. For very short time $t \ll \ell$ it reduces to the $\ell = \infty$ case Eq. (15) as it should. The leading term for $t > \ell$ is just the ground state value for a slit in an infinite line. However the subleading term is not the same, in fact we have

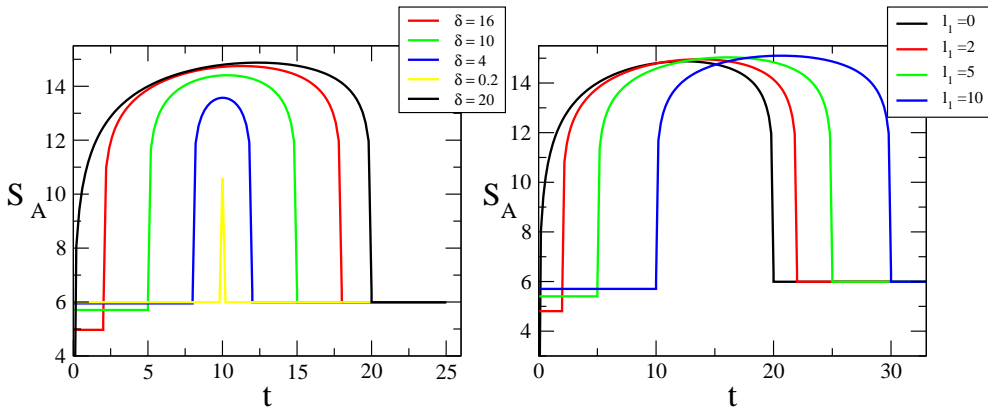
$$S_A(t > \ell) - S_A(\text{eq}) = 2\tilde{c}'_1 - c'_1 = \log g, \quad (30)$$

where we also use the value of ϵ in Eq. (16). This is a signal that for long time the system still remembers something of the initial configuration as a boundary term that is unable to “dissipate”. Since the extra energy never dissipates under unitary evolution, there is no reason for the constant terms to be the same.

Another interesting feature is the behavior for $t < \ell$. This is very similar to the form proposed in Ref. [13] to fit the numerical data, i.e.

$$S_A = \frac{c_0}{3} \log \ell + \frac{c_1}{3} \log(t/\ell) + \frac{c_2}{3} \log(1 - t/\ell) + k'. \quad (31)$$

Figure 3. $S_A(t)$ for a general slit $B = [\ell_1, \ell_2]$. The plots are done for finite $\epsilon = 10^{-3}$, and they are indistinguishable from the asymptotic result. In all the plots $\ell_1 - \ell_2 = 20$. Left: $\ell_2 < 0$, for several $\delta = \ell_1 + \ell_2$. Right: $\ell_2 > 0$, for several ℓ_1 .



Only the term in $t + \ell$ was missing in Ref. [13]. However this behaves smoothly for $0 < t < \ell$ and its effect can be well approximate by a constant factor in k' . It will be interesting to check whether and how the use of this term in $\ell + t$ changes the quality of the fit. Furthermore the fit of Ref. [13] is also a strong confirmation of our result, indeed they found $c_0 \simeq 1 + c_2$, $c_1 \simeq 1$, and $c_2 \simeq 1/2$ (plot 7 in Ref. [13] with $t' = 0$) that are exactly our predictions for $c = 1$ (the known central charge of the XX model).

Furthermore Eq. (29) display a large plateau for $0.2 < t/\ell < 0.8$ as shown in Fig. 3 (the black line in both the plots) and already noticed in Ref. [13]. This plateau can be studied considering the value at the maximum $t/\ell = (\sqrt{5} - 1)/2$ where we have

$$S_A(\text{plateau}) = \frac{c}{2} \log \frac{\ell}{a} + k_1 = \frac{3}{2} S_A(\text{eq}) + k_2, \quad (32)$$

with the constants k_p simply related to a , ϵ , and \tilde{c}'_1 .

Finally we can study the result for $t = 0$ when $\epsilon \ll \ell$:

$$S_A(t = 0) = \frac{c}{6} \log \frac{4\epsilon\ell}{a^2} + 2\tilde{c}'_1 = \frac{c}{6} \log \frac{2\ell}{a} + \tilde{c}'_1, \quad (33)$$

where in the last equality we used the value of ϵ given by Eq. (16). This result is exactly the initial value for a slit of length ℓ in the half-line. Again this is an highly non-trivial consistency check of all the method. A final curiosity is that

$$2S_A(t = 0) - S_A(t > \ell) = \frac{c}{3} \log 2, \quad (34)$$

is independent of the details of the theory.

3.4. Case IV: The general slit

Let us now consider the most general case of a slit $A = [\ell_2, \ell_1]$. In the z plane we have to calculate the two-point function between $z_1 = \ell_1 + i\tau$ and $z_2 = \ell_2 + i\tau$. Under the mapping (1) these correspond to $w_p = \ell_p + i\tau + \rho_p e^{i\theta_p}$ with ρ_p and θ_p given by Eq. (18) with $\ell \rightarrow \ell_p$ and $p = 1, 2$. In imaginary time, after a long, but straightforward algebra we have

$$\left(\frac{\langle \Phi_n(z_1 = i\tau + \ell_1) \Phi_{-n}(z_2 = i\tau + \ell_2) \rangle}{\tilde{c}_n^2} \right)^{1/x_n} = \frac{\sqrt{(\ell_1 + \rho_1 \cos \theta_1)^2 + (\tau + \rho_1 \sin \theta_1)^2} \sqrt{(\ell_2 + \rho_2 \cos \theta_2)^2 + (\tau + \rho_2 \sin \theta_2)^2}}{4\rho_1\rho_2(\ell_1 + \rho_1 \cos \theta_1)(\ell_2 + \rho_2 \cos \theta_2)} \times \frac{(\ell_1 + \ell_2 + \rho_1 \cos \theta_1 + \rho_2 \cos \theta_2)^2 + (\rho_1 \sin \theta_1 - \rho_2 \sin \theta_2)^2}{(\ell_1 - \ell_2 + \rho_1 \cos \theta_1 - \rho_2 \cos \theta_2)^2 + (\rho_1 \sin \theta_1 - \rho_2 \sin \theta_2)^2}. \quad (35)$$

The analytic continuation can be simplified for $t, \ell_1, \ell_2 \gg \epsilon$. For simplicity in the notation, but without loss of generality, we indicate as ℓ_1 the larger in absolute value of the two ℓ_p and we assume $\ell_1 > 0$. ℓ_2 can be either positive or negative. For $t < |\ell_2|$ we have a different result if the two points are on the same side or on different sides of the defect, namely:

$$S_A(t < |\ell_2|) = \begin{cases} \frac{c}{6} \log \frac{4\ell_1|\ell_2|}{a^2} + 2\tilde{c}'_1 & \ell_2 < 0, \\ \frac{c}{6} \log \frac{(\ell_1 - \ell_2)^2}{(\ell_1 + \ell_2)^2} \frac{4\ell_1\ell_2}{a^2} + 2\tilde{c}'_1 & \ell_2 > 0. \end{cases} \quad (36)$$

The first is just the sum of the entanglement entropies of two slits of length ℓ_1 and $|\ell_2|$ in the half-line starting at the origin. In fact, in the initial state the two parts

are unentangled and the total entropy is the sum of the two. Also the second result is just the ground state value for the slit $[\ell_2, \ell_1]$ in the half-line [4].

The entanglement between A and B becomes sensitive to the joining of the system when the quasiparticles emitted from the origin arrive at ℓ_2 . The behavior for $|\ell_2| < t < \ell_1$ does not depend on the relative sign of the ℓ_p :

$$S_A(|\ell_2| < t < \ell_1) = \frac{c}{6} \log \frac{(\ell_1 - \ell_2)(\ell_1 - t)}{(\ell_1 + \ell_2)(\ell_1 + t)} \frac{4\ell_1(t^2 - \ell_2^2)}{\epsilon a^2} + 2\tilde{c}'_1. \quad (37)$$

Finally for $t > \ell_1$ we have almost the ground state value:

$$S_A(t > \ell_1) = \frac{c}{3} \ln \frac{\ell_1 - \ell_2}{a} + 2\tilde{c}'_1, \quad (38)$$

that is exactly the same as for case III.

The resulting S_A for different values of ℓ_p is plotted in Fig. 3. For $|\ell_2| < t < \ell_1$ there is again a large plateau whose actual extension and value depend on both ℓ_p . The analytical value of the plateau is quite complicated and not really illuminating (it contains cubic roots, as can be realized solving the equation for the maximum). The most important features are that it decreases when the defect penetrates deeply in the slit (left part of Fig. 3) and it stays almost constant when the slit moves far from the defect (right part of the figure).

Finally one can easily read off from our formula the result for a defect exactly at the center of the slit: the entanglement entropy is independent of the time. This is different from what found numerically in a lattice model [13] and will be discussed (among the other things) in the next subsection.

3.5. Comparison with numerical works

As far as we are aware the entanglement entropy after a local quench has been discussed in only two papers [13, 26]. There are a few qualitative differences between these results and the asymptotic ones of the CFT that are easily understood in terms of the general scenario we draw for quasiparticles emitted from the origin. These differences are attributable to slow quasiparticles, that exist as consequence of a non-linear dispersion relation $v_k = \partial_k E_k$, emitted from the joining point at $t = 0$.

The first difference is that the lattice numerics present, on top of a smooth curve, very fast oscillations. These oscillations have been discussed in the context of global quenches [19, 12], and are due to the modes at the zone boundary $|ka| = \pi$ that have $v_k = 0$. However, they are only corrections to the asymptotic result for $t, \ell \gg a$, since their amplitude remains constant while the CFT result diverges. Furthermore for any specific model they can be easily predicted in a quantitative way.

In Ref. [13] different configurations of slits were considered for electron hopping on a chain (XX model in spin language). The sharp horizon effect is present even in the numerics, since there cannot be (by definition) quasiparticles faster than the CFT ones. We already discussed that the numerical results for a defect at the boundary of the slit is in *quantitative* agreement with the CFT in the region $t < \ell$. However for $t > \ell$ the numerics show an asymptotic value that appears to be exactly that of the ground state. Accordingly to our analysis this is possible only when the boundary entropy $\log g$ vanishes.

The most relevant qualitative difference is that for t greater than the maximum length the asymptotic result is not constant but it is slowly decaying (like $\log(t)/t$) smoothing the sharp transition from the plateau. This, for example, changes

completely the behavior in the case of central defect. We expect that this phenomenon can be ascribed to the slow quasiparticles that, after the quickest ones have arrived entangling the two parts, then disentangle them for very long times. This is the most plausible explanation, but we do not have an argument to put it on a more quantitative level.

4. Correlation functions

In this section we derive the time-dependence of correlation functions after the local quench. We find that the one-point function whose functional form is completely fixed by conformal invariance. The two-point functions instead depend on the particular (boundary) CFT. We will discuss all the details in the simplest case of a gaussian theory and then show how from general CFT arguments we can obtain part of the asymptotic behavior. Some of these results may have been previously derived in the context of quantum impurity problems from a different point of view (see e.g. [27]).

4.1. One-point function

The one-point function of a primary field in the half-plane $\text{Re } w > 0$ is

$$\langle \Phi(w) \rangle = \frac{A_b^\Phi}{[2\text{Re } w]^{x_\Phi}}, \quad (39)$$

where x_Φ is the scaling dimension of the field and A_b^Φ is a non-universal amplitude that can be fixed in terms of the normalization of the two-point function of the same operator. We also fix the lattice spacing a to 1. A_b^Φ is known for the simplest universality classes as the Gaussian theory and the Ising model [28].

With the mapping (9) we can get the one-point correlation, that obviously assumes the same form as Eq. (20). At the point r , after continuing to real time we have

$$\langle \Phi(r, t) \rangle = \begin{cases} A_b^\Phi (2r)^{-x_\Phi} & t < r, \\ A_b^\Phi \left(\frac{\epsilon}{2(t^2 - r^2)} \right)^{x_\Phi} & t > r. \end{cases} \quad (40)$$

Thus for short times the correlation takes its initial value, until the effect of the joining arrives at time $t = r$ when it decays for $t \gg r$ like t^{-2x_Φ} (note that this exponent is twice the boundary one).

4.2. A two-point function: the gaussian model

For the gaussian model the two-point function of a primary field Φ in the half-plane is given by Eq. (23) with $(\ell_2, \ell_1) \rightarrow (r_2, r_1)$ and $c_n \rightarrow (A_b^\Phi)^2 = 1$ [14]. As a consequence we can obtain its scaling as a byproduct of the result for the entanglement entropy for a general slit in Sec. 3.4.

For simplicity in the notation we assume here and in the following section r_1 to be positive and to be larger than the absolute value of r_2 that can be either positive or negative. Thus we have that for $t < |r_2|$ the two-point function keeps its initial value that has a different form depending on the relative signs of r_p given by $|4r_1 r_2|^{-x_\Phi}$ (different sides of the defect) and $|4r_1 r_2 (r_1 - r_2)^2 / (r_1 + r_2)^2|^{-x_\Phi}$ (same side).

For $t > r_1$, it reaches the ground state value $|r_1 - r_2|^{-2x_\Phi}$. An interesting and non-trivial behavior is displayed for $|r_2| < t < r_1$ when

$$\langle \Phi(r_1, t) \Phi(r_2, t) \rangle = \left[\frac{(r_1 + r_2)(r_2 + t)}{(r_1 - r_2)(r_1 - t)} \frac{\epsilon}{4r_1(t^2 - r_2^2)} \right]^{x_\Phi}. \quad (41)$$

4.3. The general two-point function

There are some features of the previous result that are expected to be valid in general, not only for a Gaussian theory, as for example the the horizon effect and the final equilibrated value. The natural expectation is that these results are obtainable with CFT and in fact we will show that this is the case.

The two-point function in the half-plane can be always written as [14]

$$\langle \Phi(w_1) \Phi(w_2) \rangle = \left(\frac{|w_1 + \bar{w}_2| |w_2 + \bar{w}_1|}{|w_1 - w_2| |\bar{w}_2 - \bar{w}_1| |w_1 + \bar{w}_1| |w_2 + \bar{w}_2|} \right)^{x_\Phi} F(\eta), \quad (42)$$

where η is the four-point ratio

$$\eta = \frac{|w_1 + \bar{w}_1| |w_2 + \bar{w}_2|}{|w_1 + \bar{w}_2| |w_2 + \bar{w}_1|}, \quad (43)$$

and the function $F(\eta)$ depends explicitly on the considered (boundary) model. It is known for the simplest models as e.g. the Gaussian ($F(\eta) = 1$) and the Ising universality class (see below).

Thus the behavior of the two-point function depends mainly on the value on the ratio η that we now study. Using the analytic structure of the previous section we have for $t < |r_2|$ a different behavior if the two points are on the same or on different sides of the defect:

$$\eta(t < |r_2|) = \begin{cases} \frac{4r_1 r_2}{(r_1 + r_2)^2} & r_2 > 0, \\ \frac{\epsilon^2 r_1 |r_2|}{(r_1^2 - t^2)(r_2^2 - t^2)} & r_2 < 0. \end{cases} \quad (44)$$

For intermediate times we have

$$\eta(|r_2| < t < r_1) = \frac{2r_1(r_2 + t)}{(r_1 + r_2)(r_1 + t)}, \quad (45)$$

while for larger times η is 1 constantly.

From the previous subsection we already know how the first part of Eq. (42) transforms under the conformal mapping (9). Thus we need only to map $F(\eta)$ that, in general, is an unknown function. However we know its behavior in two special circumstances. Indeed when $\eta \sim 1$ the two points are deep in the bulk, meaning $F(1) = 1$. Instead for $\eta \ll 1$, from the short-distance expansion, we have

$$F(\eta) \simeq (A_b^\Phi)^2 \eta^{x_b}, \quad (46)$$

where x_b is the boundary scaling dimension of the leading boundary operator to which Φ couples and A_b^Φ is the bulk-boundary operator product expansion coefficient that equals the one introduced in Eq. (39) [see e.g. [28]].

From this we easily understand the behavior for $t > r_1$. Since $\eta \rightarrow 1$ so $F(1) = 1$, the two-point function is just the one in the ground state

$$\langle \Phi(r_1 < t) \Phi(|r_2| < t) \rangle = \frac{1}{|r_1 - r_2|^{2x_\Phi}}. \quad (47)$$

Although this result could have been expected, it is important to have recovered it only from CFT arguments.

The behavior for $|r_2| < t < r_1$ is instead more complicated: combining the result of the previous section with the value of η we have

$$\langle \Phi(r_1, t) \Phi(r_2, t) \rangle = \left[\frac{(r_1 + r_2)(r_2 + t)}{(r_1 - r_2)(r_1 - t)} \frac{\epsilon}{4r_1(t^2 - r_2^2)} \right]^{x_\Phi} F \left(\frac{2r_1(r_2 + t)}{(r_1 + r_2)(r_1 + t)} \right). \quad (48)$$

For example when Φ is the order parameter in the Ising universality class we have [14]

$$F(\eta) = \frac{\sqrt{1 + \eta^{1/2}} \pm \sqrt{1 - \eta^{1/2}}}{\sqrt{2}}, \quad (49)$$

and $x_\Phi = 1/8$. The sign \pm depends on the boundary conditions. $+$ corresponds to fixed boundary conditions and $-$ to free ones. This completely fixes the behavior of the two-point function in the intermediate regime. It would be very interesting to check this prediction.

The time evolution for $t < |r_2|$ depends on the sign of r_2 . For $r_2 > 0$ we have

$$\langle \Phi(r_1, t) \Phi(r_2, t) \rangle = \left[\frac{1}{4r_1 r_2} \frac{(r_1 + r_2)^2}{(r_1 - r_2)^2} \right]^{x_\Phi} F \left(\frac{4r_1 r_2}{(r_1 + r_2)^2} \right), \quad (50)$$

i.e. it keeps its initial value until $t = r_2$, that is nothing but correct boundary value at zero time.

More complicated is the behavior for $r_2 < 0$, in fact we get

$$\begin{aligned} \langle \Phi(r_1, t) \Phi(r_2, t) \rangle &= \frac{1}{|4r_1 r_2|^{x_\Phi}} F \left(\frac{\epsilon^2 r_1 |r_2|}{(r_1^2 - t^2)(r_2^2 - t^2)} \right) \\ &\simeq \frac{(A_b^\Phi)^2}{|4r_1 r_2|^{x_\Phi}} \left(\frac{\epsilon^2 r_1 |r_2|}{(r_1^2 - t^2)(r_2^2 - t^2)} \right)^{x_b}, \end{aligned} \quad (51)$$

where in the last approximation we used that $\epsilon \ll t, r_1, r_2$ and the behavior of $F(\eta)$ for $\eta \ll 1$. In particular we note that this is time independent only when $x_b = 0$, which corresponds to the case of a non-zero 1-point function. Similar anomalous time-behavior was found when $x_b > 0$ in Ref. [6].

5. Decoupled finite interval

A natural question arising is how the results we just derived change when we introduce more than one defect in the line. It is straightforward to have a path integral for the density matrix: we only need to have pairs of slits for $-\infty$ to $-i\epsilon$ and from $i\epsilon$ to $+\infty$ everywhere there is a defect. However it becomes prohibitively difficult to treat this case analytically. In order to begin to understand the case when a finite interval interval is initially decoupled, we consider the case when it lies at the end of a half-line.

So, let us consider a semi-infinite chain in which the A subsystem is the finite segment $(-\ell, 0)$ and the B is the complement $(0, \infty)$ and with the initial defect at $r_D = 0$. The space-time geometry describing this situation is like the one just considered, with a wall at $-\ell + iy$ (y real) that represents the boundary condition. This is depicted in the left panel of Fig. 4.

In these circumstances the inverse conformal mapping between the z plane and the half-plane can be worked out using the Schwarz-Christoffel formula. After long algebra one obtains

$$z(w) = i \left(\frac{\ell}{\pi} \log(iw) + b \frac{-iw - 1}{-iw + 1} \right), \quad (52)$$

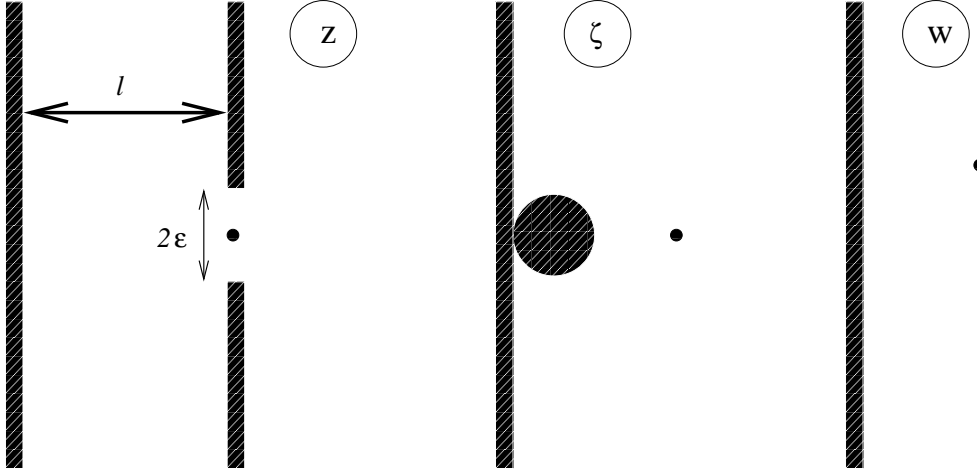


Figure 4. Left: Space-time region for the density matrix of a semi-infinite system. Center: Mapping of the z -plane under the transformation Eq. (9). Right: Final map to the half-plane of the ζ plane given by Eq. (54) when $\ell \gg \epsilon$.

with the parameter b related to ℓ and ϵ in a non-algebraic way. (A slit in the full line is closely related to this transformation, the last piece is replaced by $(w^2 - 1)/(w^2 + 1)$.) Unfortunately the mapping (52) is not analytically invertible and its exact use is limited to numerical calculations that do not help us, since we need to perform an analytical continuation. We will develop in the remaining part of the section an approximate solution for $\ell \gg \epsilon$, that however is not always justified: this limit is allowed only *after* the analytical continuation to real time.

The limit $\ell \gg \epsilon$ before the analytical continuation simplifies the calculation because under the conformal transformation (9) the boundary at $x = -\ell$ is approximately a disk tangent to the imaginary axis at the origin and with radius $R = \epsilon/4\ell \ll 1$, as depicted in the central part of Fig. 4. This is simply checked applying the inverse transformation (9) to the disk $\zeta = R(1 + e^{i\theta})$ with $\theta \in [0, 2\pi]$. In fact we have

$$z = \epsilon \frac{\zeta^2 - 1}{2\zeta} = \epsilon \frac{R^2(1 + e^{i\theta})^2(1 + e^{-i\theta}) - (1 + e^{-i\theta})}{4R(1 + \cos\theta)} = -\frac{\epsilon}{4R} - i\frac{\epsilon}{4R} \tan\theta/2 + O(R). \quad (53)$$

The half-plane minus the disk $R(1 + e^{i\theta})$ is mapped in the half-plane $\text{Re } w > 0$ by the transformation

$$w = -i \exp(2\pi i R/\zeta). \quad (54)$$

Let us note that when $\epsilon \ll \ell$, the parameter b is given by $b = \pi\epsilon^2/(8\ell) + O(\epsilon^4/\ell^2)$.

Combining the two transformations we can map the space-time region on the left of Fig. 4 into the half-plane (only in the limit $\ell \gg \epsilon$) by means of

$$w = -i \exp \left[\frac{\pi i \epsilon}{2\ell} \left(\sqrt{z^2/\epsilon^2 + 1} - z/\epsilon \right) \right], \quad (55)$$

with inverse

$$z(w) = i\frac{\ell}{\pi} \log(iw) + i\frac{\epsilon^2}{\ell} \frac{\pi}{4} \frac{1}{\log(iw)}. \quad (56)$$

Note that the residue of the pole at $w = -i$ is the same as the exact one in Eq. (52). Furthermore, calculating the the difference between the approximate and the exact solution, one easily checks that it is of the order of ϵ^4/ℓ^2 everywhere in the complex plane.

We then have that $w(i\tau)$ can be written as

$$w(i\tau) = -ie^{\pi\tau/2\ell} \left[\cos(\sqrt{1 - \tau^2/\epsilon^2}\pi\epsilon/2\ell) + i \sin(\sqrt{1 - \tau^2/\epsilon^2}\pi\epsilon/2\ell) \right]. \quad (57)$$

Thus

$$\langle \Phi_n(i\tau) \rangle = \tilde{c}_n \left[\frac{\pi\epsilon}{4\ell} \frac{1}{\sqrt{\epsilon^2 - \tau^2}} \frac{1}{\sin(\pi\sqrt{\epsilon^2 - \tau^2}/2\ell)} \right]^{x_n}. \quad (58)$$

Note that for $\ell \rightarrow \infty$ it reduces to the previous result, as it should. Furthermore, it is clear that it is well defined only for $\ell \gg \epsilon$.

Continuing to real time $\tau \rightarrow it$, and for $t \gg \epsilon$ we have

$$\langle \Phi_n(it) \rangle = \tilde{c}_n \left[\frac{\pi\epsilon}{4\ell} \frac{1}{t \sin(\pi t/2\ell)} \right]^{x_n}. \quad (59)$$

Clearly this cannot make sense when the argument of the power-law becomes negative (i.e. for $t > 2\ell$), signaling that there is something wrong in the derivation. However, using the replica trick, for the entanglement entropy we obtain

$$S_A = \frac{c}{6} \log \left(\frac{4\ell}{\pi\epsilon} t \sin(\pi t/2\ell) \right) + \tilde{c}'_1. \quad (60)$$

One is tempted to assume that this result can be correct only for $t < \ell$ and that for larger time it saturates as suggested by the quasiparticle interpretation. Only an exact calculation via the exact mapping (52) can resolve these doubts. However exact solutions of integrable models or numerical density matrix renormalization group could already be able to eventually exclude Eq. (60) and to shed some light on the problem. We mainly mention this topic here to encourage further studies in this direction.

Finally let us point out that transformations similar to Eq. (52) appear when studying finite-size effects.

6. Discussion

We presented a detailed study of the unitary evolution that results after a local quench in a quantum one-dimensional system. All our findings have been obtained by means of CFT and so they are limited to the evolution of a gapless quantum model with a linear dispersion relation. We presented calculations for the entanglement entropies for different bipartitions of the system and for one- and two-point correlation functions in a general CFT. In particular we studied the case when two half-systems are joined at time $t = 0$.

All our results are interpretable in terms of a scenario that we believe to be valid in general, not only for gapless systems (in analogy to the case of global quenches [6, 19, 12]). In fact, the initial state is expected to generate quasiparticle excitations at $r_D = 0$ that then propagate freely through the system and carry all the information about entanglement and correlations. In the case of a CFT all these excitations travel at the same speed v_s ($= 1$ by normalization). However in general, as a consequence of a non-linear dispersion relation, a full spectrum of velocities is expected.

Although the physical cut may seem a rather specific situation, we believe that our findings are quite general. For example, a general defect (e.g. a weakened bond)

is asymptotically equivalent to the results we obtained here as long as the defect is a relevant perturbation. This excludes the XX chain that is the only model studied so far [13], where the defect is believed to be marginal [29], but should apply to XXZ spin-chains [30]. Furthermore we expect a qualitatively similar behavior when a system has been artificially prepared in a configuration that is only locally different from the ground state. For example there are already several studies where the local horizon effect is evident (see e.g. those considered in Refs. [31]). A full quantitative analysis of most of these settings should be possible properly adapting our CFT treatment (e.g. with the theory of boundary condition changing operators [24]). On the other hand, also the case of an initial state with one or more kinks displays a time-evolution with an horizon effect similar to the one considered here (see e.g. Refs. [32] where also finite temperature results are obtained in a rigorous manner). It would be interesting to understand whether these results can be recovered analytically continuing some CFT results. Work in this direction is in progress.

We described here several different physical situations, but many problems are still left for future investigations. A first goal would be to check our predictions in exactly solvable models. In fact, as far as we are aware only the paper by Eisler and Peschel [13] discussed these topics in the context of the XX model and their results are fully compatible with ours.

Another simple generalization of our results is to study gapped exactly solvable models, like the Ising model in a transverse magnetic field or others admitting a free-field representation. In these case it is also interesting to understand whether some predictions can be made on the basis of the generalized Gibbs ensemble [33].

A more difficult question to study analytically concerns the role played by quenched disorder. This is expected to change at a qualitative level the quasiparticle scenario as a consequence of Anderson localization [34]. In this case the time-dependent density matrix renormalization group [35] should be quite effective, since for clean systems we know that the entanglement entropy never increases dramatically as it does in the case of global quenches.

Acknowledgments

This work was supported in part by EPSRC grants GR/R83712/01 and EP/D050952/1. This work has been done in part when PC was a guest of the Institute for Theoretical Physics of the Universiteit van Amsterdam. This stay was supported by the ESF Exchange Grant 1311 of the INSTANS activity. PC thanks Dragi Karevski for useful discussions.

References

- [1] L. Amico, R. Fazio, A. Osterloh, and V. Vedral, Entanglement in Many-Body Systems, quant-ph/0703044.
- [2] C. Holzhey, F. Larsen, and F. Wilczek, Geometric and Renormalized Entropy in Conformal Field Theory, Nucl. Phys. B **424**, 443 (1994) [hep-th/9403108]
- [3] G. Vidal, J. I. Latorre, E. Rico, and A. Kitaev, Entanglement in quantum critical phenomena, Phys. Rev. Lett. **90**, 227902 (2003) [quant-ph/0211074]
J. I. Latorre, E. Rico, and G. Vidal, Ground state entanglement in quantum spin chains, Quant. Inf. and Comp. **4**, 048 (2004) [quant-ph/0304098]
- [4] P. Calabrese and J. Cardy, Entanglement entropy and quantum field theory, J. Stat. Mech. P06002 (2004) [hep-th/0405152]

- [5] J. L. Cardy, O.A. Castro-Alvaredo, and B. Doyon, Form factors of branch-point twist fields in quantum integrable models and entanglement entropy, arXiv:0706.3384.
- [6] P. Calabrese and J. Cardy, Evolution of Entanglement entropy in one dimensional systems, *J. Stat. Mech.* P04010 (2005) [cond-mat/0503393].
- [7] G. De Chiara, S. Montangero, P. Calabrese, and R. Fazio Entanglement Entropy dynamics in Heisenberg chains, *J. Stat. Mech.* P03001 (2006) [cond-mat/0512586]
- [8] J. Eisert and T. J. Osborne, General Entanglement Scaling Laws from Time Evolution, *Phys. Rev. Lett.* **97**, 150404 (2006) [quant-ph/0603114];
S. Bravyi, M. B. Hastings, and F. Verstraete, Lieb-Robinson Bounds and the Generation of Correlations and Topological Quantum Order, *Phys. Rev. Lett.* **97**, 050401 (2006) [quant-ph/0603121].
- [9] L. Cincio, J. Dziarmaga, M. M. Rams, W. H. Zurek, Entropy of entanglement and correlations induced by a quench: Dynamics of a quantum phase transition in the quantum Ising model, *Phys. Rev. A* **75**, 052321 (2007) [cond-mat/0701768].
- [10] V. E. Hubeny, M. Rangamani, T. Takayanagi, A Covariant Holographic Entanglement Entropy Proposal, *JHEP* P07062 (2007) [arXiv:0705.0016].
- [11] M. Greiner, O. Mandel, T. W. Hänsch, and I. Bloch, Collapse and Revival of the Matter Wave Field of a Bose-Einstein Condensate, *Nature (London)* **419**, 51 (2002) [cond-mat/0207196]
L. E. Sadler, J. M. Higbie, S. R. Leslie, M. Vengalattore, and D. M. Stamper-Kurn, Spontaneous symmetry breaking in a quenched ferromagnetic spinor Bose-Einstein condensate, *Nature* **443**, 312 (2006)
T. Kinoshita, T. Wenger, and D. S. Weiss, A quantum Newton's cradle, *Nature* **440**, 900 (2006)
A. Widera, F. Gerbier, S. Fölling, T. Gericke, O. Mandel, and I. Bloch, Coherent Collisional Spin Dynamics in Optical Lattices, *Phys. Rev. Lett.* **95**, 190405 (2005).
- [12] P. Calabrese and J. Cardy, Quantum Quenches in Extended Systems, *J. Stat. Mech.* P06008 (2007) [arXiv:0704.1880].
- [13] V. Eisler and I. Peschel, Evolution of entanglement after a local quench, *J. Stat. Mech.* P06005 (2007) [cond-mat/0703379].
- [14] J. L. Cardy, Conformal Invariance and Surface Critical Behavior, *Nucl. Phys. B* **240**, 514 (1984)
- [15] J. L. Cardy, Boundary Conformal Field Theory, in *Encyclopedia of Mathematical Physics*, ed J.-P. Francoise, G. Naber, and S. Tsou Tsou, (Elsevier, Amsterdam, 2006).
- [16] I. Affleck and A. W. W. Ludwig, Universal non-integer "ground-state degeneracy" in critical quantum systems, *Phys. Rev. Lett.* **67**, 161 (1991).
- [17] H.-Q. Zhou, T. Barthel, J. O. Fjærestad, and U. Schollwoeck, Entanglement and boundary critical phenomena. *Phys. Rev. A* **74**, 050305(R) (2006) [cond-mat/0511732].
- [18] N. Laflorencie, E. S. Sorensen, M.-S. Chang, and I. Affleck, Boundary effects in the critical scaling of entanglement entropy in 1D systems, *Phys. Rev. Lett.* **96**, 100603 (2006) [cond-mat/0512475]
- [19] P. Calabrese and J. Cardy, Time-dependence of correlation functions following a quantum quench, *Phys. Rev. Lett.* **96**, 136801 (2006) [cond-mat/0601225].
- [20] M. A. Cazalilla. Effect of suddenly turning on the interactions in the Luttinger model, *Phys. Rev. Lett.* **97**, 156403 (2006) [cond-mat/0606236].
- [21] A. Lamacraft, Quantum quenches in a spinor condensate, *Phys. Rev. Lett.* **98**, 160404 (2007) [cond-mat/0611017].
- [22] M. Cramer, C. M. Dawson, J. Eisert, and T. J. Osborne, Quenching, relaxation, and a central limit theorem for quantum lattice systems, cond-mat/0703314.
- [23] N. Schuch, M. M. Wolf, F. Verstraete, and J. I. Cirac, Entropy scaling and simulability by Matrix Product States, arXiv:0705.0292.
- [24] I. Affleck and A. W. W. Ludwig, The Fermi edge singularity and boundary condition changing operators, *J. Phys. A* **27**, 5375 (1994) [cond-mat/9405057].
- [25] H. W. Diehl, The theory of boundary critical phenomena, in *Phase Transitions and Critical Phenomena* vol 10 ed C Domb and J L Lebowitz (1986, London: Academic)
H. W. Diehl, The theory of boundary critical phenomena, *Int. J. Mod. phys. B* **11**, 3503 (1997) [cond-mat/9610143]
- [26] D. Gobert, C. Kollath, U. Schollwoeck, and G. Schuetz Real-time dynamics in spin-1/2 chains with adaptive time-dependent DMRG, *Phys. Rev. E* **71**, 036102 (2005) [cond-mat/0409692]
- [27] H. Saleur, Lectures on Non Perturbative Field Theory and Quantum Impurity Problems, cond-mat/9812110.
- [28] J. Cardy and D. Lewellen, Bulk and Boundary Operators in Conformal Field Theory, *Phys. Lett. B* **259**, 274 (1991).

- [29] I. Peschel, Entanglement entropy with interface defects *J. Phys. A: Math. Gen.* **38**, 4327 (2005) [cond-mat/0502034].
- [30] J. Zhao, I. Peschel, and X. Wang Critical entanglement of XXZ Heisenberg chains with defects, *Phys. Rev. B* **73**, 024417 (2006) [cond-mat/0509338]
G. Levine, Entanglement entropy in a boundary impurity model, *Phys. Rev. Lett.* **93** 266402 (2004) [cond-mat/0408366].
- [31] L. Amico, A. Osterloh, F. Plastina, R. Fazio, and G. M. Palma, Dynamics of Entanglement in One-Dimensional Spin Systems, *Phys. Rev. A.* **69**, 022304 (2004) [quant-ph/0307048]
C. Kollath, U. Schollwck, J. von Delft, and W. Zwerger, One-dimensional density waves of ultracold bosons in an optical lattice, *Phys. Rev. A* **71**, 053606 (2005) [cond-mat/0411403]
C. Kollath, U. Schollwoeck, and W. Zwerger, Spin-charge separation in cold Fermi-gases: a real time analysis, *Phys. Rev. Lett.* **95**, 176401 (2005) [cond-mat/0504299]
T. S. Cubitt and J. I. Cirac, Engineering correlation and entanglement dynamics in spin systems, quant-ph/0701053.
M. Polini and G. Vignale, Spin Drag and Spin-Charge Separation in Cold Fermi Gases, *Phys. Rev. Lett.* **98**, 266403 (2007) [cond-mat/0702466]
- [32] T. Antal, Z. Racz, A. Rakos, and G. M. Schutz, Transport in the XX chain at zero temperature: Emergence of flat magnetization profiles, *Phys. Rev. E* **59**, 4912 (1999) [cond-mat/9812237];
D. Karevski, Scaling behaviour of the relaxation in quantum chains, *Eur. Phys. J. B* **27**, 147 (2001) [cond-mat/0203078];
Y. Ogata, Diffusion of the Magnetization Profile in the XX-model, *Phys. Rev. E* **66**, 066123 (2002) [cond-mat/0210011];
W. H. Aschbacher and C.-A. Pillet, Non-equilibrium steady states of the XY chain, *J. Stat. Phys.* **112**, 1153 (2003);
T. Platini and D. Karevski, Scaling and front dynamics in Ising quantum chains, *Eur. Phys. J. B* **48**, 225 (2005) [cond-mat/0509594];
W. H. Aschbacher and J.-M. Barbaroux, Out of equilibrium correlations in the XY chain, *Lett. Math. Phys.* **77**, 11 (2006);
T. Platini and D. Karevski, Relaxation in the XX quantum chain, *J. Phys. A* **40**, 1711 (2007) [cond-mat/0611673];
W. H. Aschbacher, Non-zero entropy density in the XY chain out of equilibrium, *Lett. Math. Phys.* **79**, 1 (2007).
- [33] M. Rigol, V. Dunjko, V. Yurovsky, and M. Olshanii, Relaxation in a Completely Integrable Many-Body Quantum System: An Ab Initio Study of the Dynamics of the Highly Excited States of Lattice Hard-Core Bosons, *Phys. Rev. Lett.* **98**, 50405 (2007) [cond-mat/0604476].
M. Rigol, V. Dunjko, and M. Olshanii, Thermalization and its mechanism for generic isolated quantum systems, arXiv:0708.1324.
- [34] C. K. Burrell and T. J. Osborne, Bounds on Information Propagation in Disordered Quantum Spin Chains, quant-ph/0703209.
P. W. Anderson, Absence of Diffusion in Certain Random Lattices, *Phys. Rev.* **109**, 1492 (1959).
- [35] A. J. Daley, C. Kollath, U. Schollwoeck, and G. Vidal, Time-dependent density-matrix renormalization-group using adaptive effective Hilbert spaces, *J. Stat. Mech.* P04005 (2004) [cond-mat/0403313];
S. R. White and A. E. Feiguin, Real time evolution using the density matrix renormalization group, *Phys. Rev. Lett.* **93**, 076401 (2004) [cond-mat/0403310].